graphene oxide, semiconductors have been employed to conduct electrocatalytic H_2O_2 detection due to their desirable chemical, physical and electronic properties that are different from those of bulk materials[10-14].

Recently, dendrimers encapsulated metal nanoparticles and dendrimer-cored metal nanoparticles have gained much attention due to their potential use in catalysis[15-23]. The advantage of dendrimer encapsulation or stabilization of nanoparticles is it minimizes the agglomeration, resulting in a controlled size of nanoparticles which enhances the activity and selectivity of the catalyst. Further, the dendrimer branches can be used as selective gates to control access of small molecules like H_2O_2 to the encapsulated nanoparticles. The dendrimer encapsulated nanoparticles can be deposited onto electrode surfaces and then used for catalysis, sensing of molecules, etc.

Metal nanoparticles are attractive to use as catalysts due to high surface-to-volume ratio and their high surface energy, which makes their surface atoms active. A H_2O_2 sensor based on a PdNPs supported on hyperbranched poly (ethylene glycol)-block-poly(citric acid)-functionalized Fe_3O_4 MNPs (Pd@ PCA-b-PEG-Fe_3O_4) modified GCE was reported to have high sensitivity and stability[24]. Elancheziyan *et al.*, reported that viologen terminated second (G2.0) and third generation (G3.0) poly(amidoamine) PAMAM dendrimers, followed by encapsulation with gold nanoparticles modified GCE as an efficient nanosensor for reduction of H_2O_2[25]. Baghayeri *et al.*, reported magnetic graphene oxide functionalized with amine-terminated poly(amidoamine) dendrimer, decorated with palladium nanoparticles (GO-Fe_3O_4-PAMAM-Pd) as an non-enzymatic electrochemical sensor for the determination of hydrogen peroxide (H_2O_2) with high sensitivity and selectivity[26]. Prussian blue (PB) is known as an artificial peroxidase comprises mixed valence inorganic complex and shows molecular sieve zeolite structure[27]. Till now, various PB based electrochemical sensing platforms have been reported for the determination of organic, inorganic and biomolecules, such as hydrogen peroxide, nitrite, glucose, and proteins due to its reversible electron transfer, good redox activity, and excellent electrocatalytic activity[28-30]. Unfortunately, PB shows poor cycling stability on the electrode surface in neutral or alkaline environments due to decomposition by hydrolysis, which significantly limits the application of PB. To overcome this, it is essential to introduce advanced material-based platforms to stabilize PB nanoparticles, such as dendrimers[31], metal nanoparticle[32], metal sulphides[33].

Considering the advantages from Prussian blue nanoparticles and dendrimers as excellent stabilizing agents, in the present work, we have fabricated a novel electrochemical sensor for sensing of hydrogen peroxide based on Prussian blue nanoparticles (PBNPs) loaded on a glassy carbon electrode (GCE) modified with amphiphilic poly(propylene imine) dendrimer (PBNPs/APPI(G3)/GCE). Its electrochemical behaviour was characterized by cyclic voltammetry and chronoamperometric studies. The obtained results showed that PBNPs/ APPI(G3)/GCE is effectively electrocatalyze the hydrogen peroxide. Further studies to improve the performance of the electrocatalyst is in progress by modifying the electrode material doped with different nanomaterials viz., carbon nanotubes, graphenes and metal oxide nanoparticles etc.

Experimental Section

Materials

Poly(propylene imine) generation-3 (G3) dendrimer (with diaminobutane core and 16 peripheral–NH2 groups was purchased from SyMO-Chem, Netherland. monobasic sodium phosphate, dibasic sodium phosphate, potassium chloride, ferrous sulphate, potassium ferricyanate were purchased from SRL, India.1,2-epoxyhexane, HPLC water, hydrogen peroxide and all other reagents were of analar grade of 99% purity and used as received.

Characterization

The UV-Vis spectra were measured on Perkin-Elmer Lambda-35 instrument with UV WinLab software. The measurements were carried out in the wavelength range of 200-800 nm under ambient conditions. The Fourier transform infrared (FT-IR) spectra were recorded in the range of 4000 to 400 cm^{-1} on a Bruker Tensor-27 FT-IR spectrophotometer with OPUS software. In general, the samples obtained from different preparation methods were quantitatively analyzed. The test sample including amphiphilic dendrimers and KBr were taken in the ratio 1:1, and then the pellet was prepared. The thickness of the pellet was measured uniformly with a dilatometer and then the analysis was performed. The ^{1}H and ^{13}C NMR spectra were recorded on a Bruker NMR spectrometer with 300 and 75 MHz respectively, using TMS as an internal standard. The thermo gravimetric analysis was also performed quantitatively by taking the same weight of the amphiphilic dendrimer templates in an SDT Q600

V20.5 Build 15 instrument at a heating rate of 10°C/min from 50 to 800°C under a nitrogen atmosphere. MALDI-TOF MS was recorded on a Voyager-DE PRO Biospectrometry workstation equipped with 337 nm N_2 laser source. All mass spectra were obtained averaging of 100 shots with negative ion mode and in reflection mode. Dithranol was used as a matrix to analyze the amphiphilic dendrimers. Analyte solution was prepared by mixing the 1 µL dendrimer solution (1 mg/1 mL methanol) and 1 µL of matrix solution (10 mg/1 mL methanol). Subsequently, 0.5 µL of this mixture was spotted on a stainless steel probe tip, and the spots were allowed to dry at room temperature. All data were processed using Voyager Version 5 Software with Data Explorer. The level of hydrophobicity of amphiphilic dendrimer templates was determined by measuring the contact angle using a Kruss Easy drop goniometer (KRUSS, DSA II GmbH, Germany). A drop of ultra-pure water (2 µL) was placed on the surface of each dendrimer template and the angle formed at the solid-liquid interface was measured directly from the photographic image, and the observed values are mentioned in each photograph. The surface morphology study was carried out on a HITACHISU6600 field emission-scanning electron microscope (FE-SEM).The samples were spread on the surface of double sided adhesive tape, one side of which was already adhered to surface of a circular copper disc pivoted by a rod. Cyclic voltammetry (CV) and amperometric *i-t* experiments were carried out with a CHI 1130A electrochemical workstation (USA). The three-electrode system consists of glassy carbon (GC) as a (3 mm dia) working electrode, Ag/AgCl with 3 M KCl as a reference electrode and platinum wire as a counter electrode with 10 mL working volume.

Synthesis of amphiphilic poly(propylene imine)-G3 dendrimer using 1,2-epoxyhexane

The synthesis of amphiphilic poly(propylene imine) dendrimer was prepared by modifying the Zhang *et al.* procedure (Scheme 1)[34]. To describe briefly, 2 mL of 1,2-epoxyhexane (4.74 mmol) was added drop wise to a 50 mL RB flask containing 0.15 mmol of PPI (G3) dissolved in 10 mL of methanol under vigorous stirring. The resulting mixture was stirred with magnetic stirrer for 3 days at ambient temperature and then it was refluxed for 1hr. The methanol and unreacted 1,2-epoxyhexane were removed by rotary evaporator, and the resulting product was dried in a vacuum to yield the

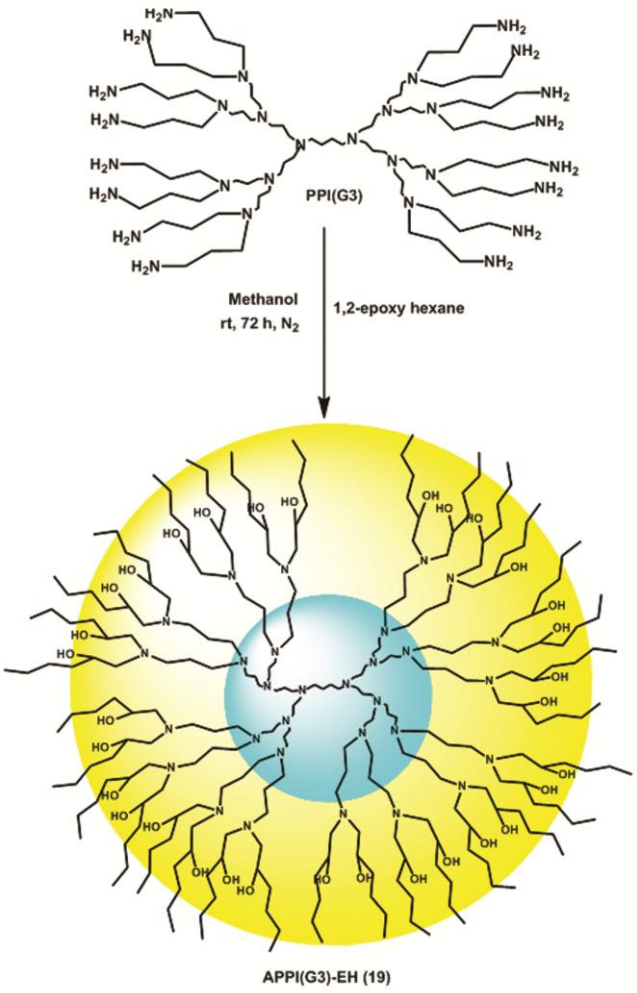

Scheme 1 — Synthesis of APPI(G3)-EH dendrimer template.

amphiphilic poly(propylene imine) dendrimer template *viz.*, APPI(G3)-EH as a viscous oil. FTIR (KBr, cm^{-1}) : 3449 (O-H str), 2932 & 2863 (C-H str), 1376 (C-H rock), 1078 (C-N str); ^{1}H NMR ($CDCl_3$, 300 MHz,): δ 0.82 (-C<u>H</u>$_3$), 1.25, 1.28 & 1.54 (-C<u>H</u>$_2$), 3.5 (-O<u>H</u>); ^{13}C NMR ($CDCl_3$, 75 MHz,): δ 14.09 (-<u>C</u>H$_3$), 22.87 (-<u>C</u>H$_2$), 34.75 (-N-<u>C</u>H$_2$), 27.92 (-OH-<u>C</u>H$_2$) and MALDI-TOF MS: Calcd: 4891.94 Found: 4885.58

Synthesis of APPI(G3)-EH dendrimer stabilized Fe^{2+}complex (APPI(G3)-Fe^{2+})

The APPI(G3)-EH was used as template and prepared the homogenous form of Prussian blue nanoparticle catalyst (PBNPs). Initially, 0.5 mmol of (24.5 mg) APPI(G3)-EH was taken in 25 mL RB, and dissolved the same in 10 mL deionized water. To that, 1.5 mmol (41.7 mg) of aqueous $FeSO_4.7H_2O$ was added drop wise under vigorous stirring. The resulting

mixture was stirred using a magnetic stirrer at ambient temperature for 24 h. The obtained colloidal dispersion was labelled as APPI(G3)-EH-Fe^{2+} and thus used for the preparation of PBNPs.

Electrochemical deposition of Prussian blue on APPI(G3)-EH-Fe^{2+}/GC modified electrode

The electrochemical deposition of PB on APPI(G3)-EH-Fe^{2+}/GC modified electrode was performed as given in (Scheme 2) Prior to the fabrication, GCE was polished with 1.0, 0.3 and 0.05 µM alumina slurries followed by rinsing with double distilled water, and then cycling between a potential range from -0.2 to +1 V at a scan rate of 50 mV/s in 0.1 M HCl and 0.1 M KCl medium. Then, the APPI(G3)-EH-Fe^{2+}/GC electrode was fabricated by drop coating method i.e., 10 µL of concentrated dispersion of APPI(G3)-EH-Fe^{2+} was uniformly coated on GCE using micropipette. Then, the solvent was allowed to evaporate at room temperature in air for 1 h.

The electrodeposition of PBNPs were achieved by immersing the APPI(G3)-EH-Fe^{2+}/GC electrode in a carefully deoxygenated (30 min) solution containing 1.5 mmol $K_3Fe(CN)_6$, 0.1M HCl and 0.1M KCl medium, followed by a cyclic scan in a potential range from -0.2 to +1 V at a scan rate of 50 mV/s for 40 cycles. After deposition, the modified electrode were thoroughly washed with double distilled water, then transferred into a supporting electrolyte solution (0.1M HCl and 0.1M KCl) and electrochemically activated by cycling between -0.2 to +1 V (60 cycles) at a scan rate of 50 mV/s.

Electrocatalytic activity of modified electrode viz., APPI(G3)-EH-PBNPs/GCE for the reduction of H_2O_2

In order to check the electrocatalytic activity of APPI(G3)-EH-PBNPs/GC electrode towards hydrogen peroxide reduction, the voltammetric responses were recorded in the absence and presence of different concentration of H_2O_2 (Scheme 3). The cyclic voltammograms of the APPI(G3)-EH-PBNPs/GC electrode in 0.1M HCl and 0.1M KCl with and without H_2O_2 shown that with the gradual addition of H_2O_2, the reduction peak current for Prussian blue was increased and the oxidation peak current decreased gradually, which indicates the catalytic properties of modified electrode to the reduction of H_2O_2. All the experiments were carried out with GC and modified electrode by fixing the potential range at -0.2 to +1 V vs Ag/AgCl in 0.1M HCl and 0.1M KCl solution at scan rate of 50 mV/s. Electrochemical sensing of H_2O_2 on the electrode surface was performed using amperometric*i-t* mode of analysis by keeping the applied potential at +0.2V at regular time intervals under continuous stirring.

Results and Discussion

Synthesis of amphiphilic dendrimer viz., APPI(G3)-EH

The structure of APPI(G3)-EH was confirmed by various spectral and analytical techniques such as

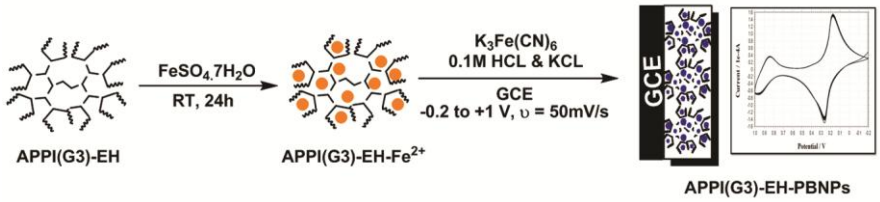

Scheme 2 — Electrochemical deposition of PBNPs on APPI(G3)-EH-Fe^{2+}/GC electrode.

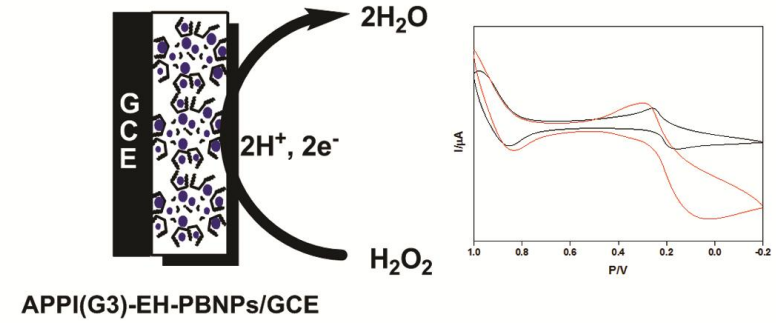

Scheme 3 — Electrocatalytic activity of APPI(G3)-EH-PBNPs/GC electrode for the reduction of H_2O_2.

FT-IR, ^{1}H & ^{13}C NMR, TGA and MALDI-TOF. The FT-IR spectra of APPI(G3)-EH and PPI(G3) (control) are shown in Fig. 1(a) and Fig. 1(b) respectively. The appearance of doublet at 3360 and 3278 cm^{-1} is attributed to the N-H stretching vibrations present in the PPI(G3) dendrimer. In contrast, in APPI(G3)-EH spectrum, this N-H_{str} disappeared and the appearance of -OH_{str} at 3449 cm^{-1} was noticed. Further, high intense peaks appeared at 2930 and 2862 cm^{-1}, due to C-H symmetric and antisymmetric stretching vibrations, respectively. The appearance of these characteristic peaks confirms the attachment of 1,2-epoxyhexane with peripheral amine groups of PPI(G3) dendrimer.

The ^{1}H NMR spectrum shows a peak at 3.53 ppm corresponding to –OH group present in the modified dendrimer [Fig. 2(a)]. Another broad multiplet was observed in the range of 1.25-1.54 ppm due to $–CH_2$-CH_2- groups present in modified dendrimer moiety. The spectrum also shows a triplet at 0.82 ppm and it is attributed to $–CH_2$-$\underline{CH_3}$ in APPI(G3)-EH dendrimer template. Similarly, in ^{13}C NMR [Fig. 2(b)] a peak at 14.09 ppm for methyl carbon and 22.87, 27.92, and 34.75 ppm for methylene carbons were noticed and this indicates the APPI(G3)-EH dendrimer. These spectral results strongly confirm the incorporation of modified epoxyhexane into the dendrimer.

Synthesis and characterization of amphiphilic dendrimer stabilized prussian blue nanoparticle catalyst viz., APPI(G3)-EH-PBNPs

In the last two decades, coating of electrode surfaces with various electro-active materials is an interesting area of research in designing and fabricating various electrochemical sensors. There are several organic and inorganic modifiers already employed to fabricate the electrodes to make them electrochemically active[35,36]. The modifiers which are already used are tungsten oxide (WO_3) and Prussian blue (PB)[37]. PB is known as "artificial enzyme peroxidase", since it can perform the electrocatalytic reduction of hydrogen peroxide at low potentials with remarkable activity and selectivity[38]. The use of nanoparticles can improve the analytical performance for hydrogen peroxide detection; nano-sized particles have unique physical and chemical properties, often showing very interesting peculiarities unmatched by their bulk counterpart. The large surface-to-volume ratio and the increased surface activity of nanoparticles, when compared to those of bulk materials, enable their use in catalysis and sensing.

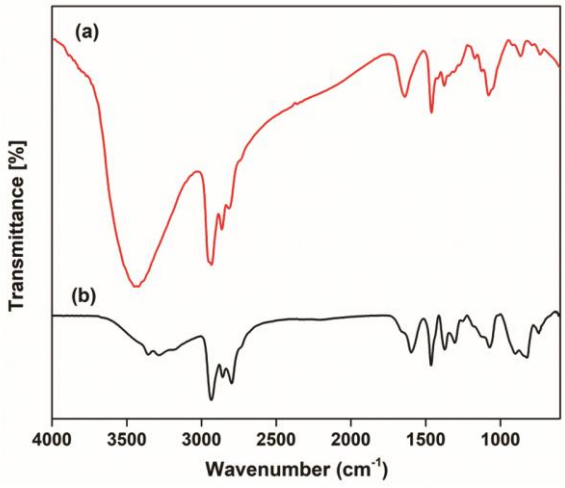

Fig. 1 — FTIR spectra of (a) APPI(G3)-EH and (b) PPI-G3.

Taking these factors into consideration, in the present study, a novel route to synthesize the Prussian blue nanoparticles using simplified amphiphilic dendrimer molecule viz., APPI(G3)-EH as stabilizing agent via electro-deposition method. In the fabrication process, initially, Fe^{2+} ion was complexed with APPI(G3)-EH dendrimer template to give APPI(G3)-EH-Fe^{2+} complex. This complex in turn was coated on GCE by placing a drop of the same solution on to the surface of GC electrode. Finally, the APPI(G3)-EH-Fe^{2+}/GC electrode was cycled between -0.2 to 1V at a scan rate of 0.1Vs^{-1} in acidic $K_3[Fe(CN)_6]$ solution as background electrolyte and thus produced APPI(G3)-EH-PBNPs/GCE. The slow dissociation of ferricyanide should be the main source of ferric ions for forming PB nanoparticles, i.e. $Fe(CN)_6^{3-} + 6H^{+} \Leftrightarrow Fe^{3+} + 6HCN\uparrow$. The PB nanoparticles are electrochemically formed according to the mechanism reported previously[39], i.e.:

$$Fe^{3+} + e^{-} \rightarrow Fe^{2+} \quad ...(1)$$

$$Fe(CN)_6^{3-} + e^{-} \rightarrow Fe(CN)_6^{4-}\ Fe(CN)_6^{4-} + H^{+} \rightarrow Fe^{2+} + HCN \quad ...(2)$$

$$xFe(CN)_6^{4-} + xFe^{3+} \rightarrow Fe_x[Fe(CN)_6]x \quad ...(3)$$

Furthermore, at the driving force of voltage, more $Fe(CN)_6^{3-}$ ions are adsorbed onto the amphiphilic dendrimers with the proceeding of electrodeposition of PBNPs. The formation of PBNPs on to the surface of GCE was characterized by cyclic voltammetry (CV) and FESEM analyses. The cyclic voltammograms of APPI(G3)-EH-PBNPs/GC electrode was investigated in 20 mL of 0.1 M KCl prepared using 0.1 M HCl solution and the growth process of the PBNPs is shown in Fig. 3. Two pairs of redox waves appeared at a formal potential ($E^{o'}$) of

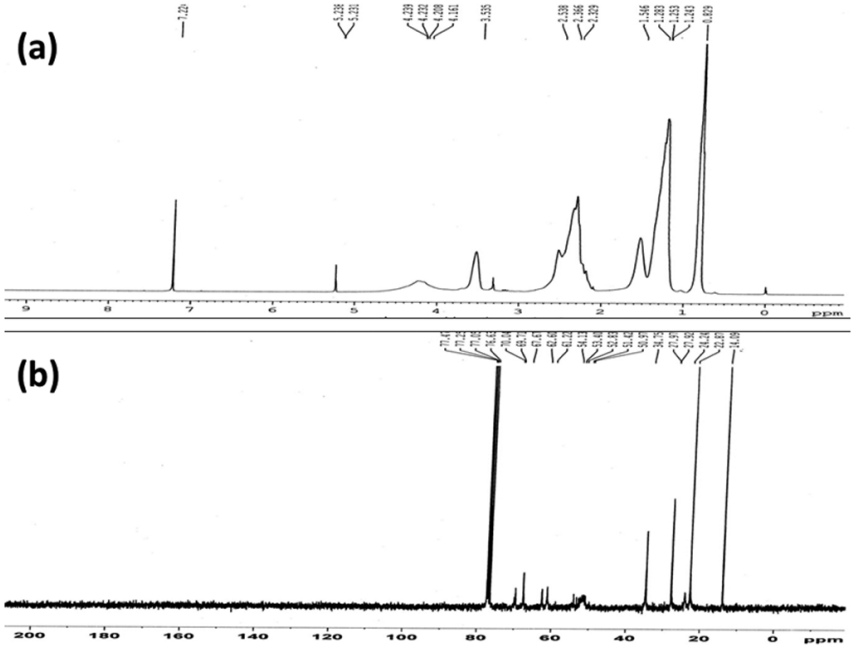

Fig. 2 — (a) ^{1}H NMR and (b) ^{13}C spectra of APPI(G3)-EH

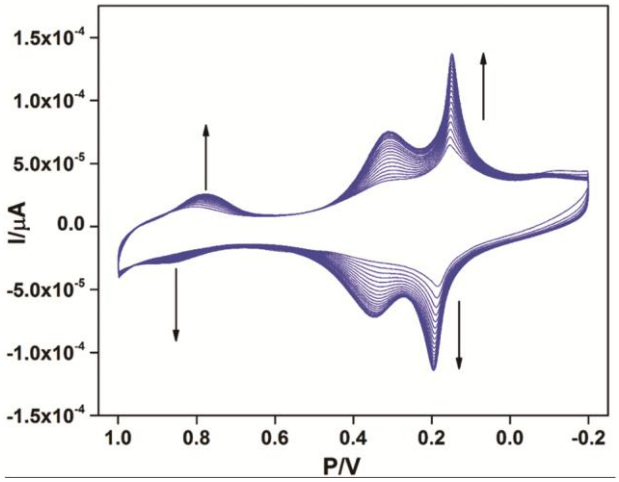

Fig. 3 — Growth process of PBNPs on the APPI(G3)-EH-Fe^{2+} coated GCE in a solution of $K_3[Fe(CN)_6]$, 0.1 M HCl/KCl at a scan rate of 50 mVs^{-1}.

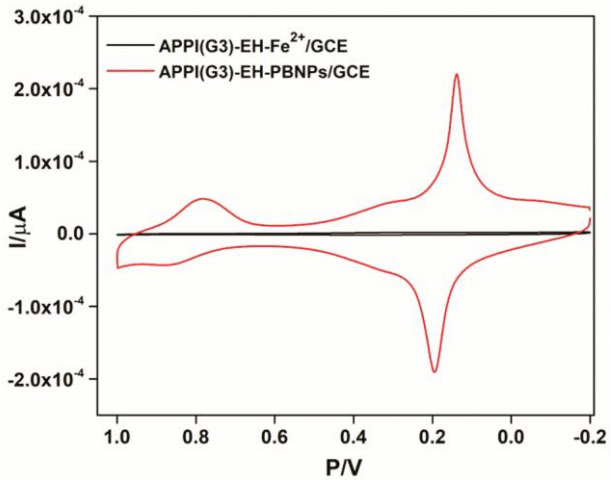

Fig. 4 — Cyclic voltammograms of modified GCE in 0.1M HCl/KCl at a scan rate of 50 mVs^{-1}.

0.172 V and 0.82 V. All the redox peaks gradually grew and the peak potentials remained relatively constant with increasing rate of the scan cycle. These phenomena demonstrated that the PBNPs had uniformly formed on the surface of the APPI(G3)-EH-Fe^{2+}/GC electrode.

After activation and stabilization, APPI(G3)-EH-PBNPs/GCE was examined in the blank electrolyte containing 0.1 M HCl/KCl, and the resulting CV curve is shown in Fig. 4. It is seen that the CV of APPI(G3)-EH-Fe^{2+}/GC electrode does not show any redox peak, due to lack of redox-active material on the electrode surface. However, after electrodeposition of PB onto the APPI(G3)-EH-Fe^{2+}/GC electrode, two pairs of typical redox waves were observed and this is due to oxidation of PB to Berlin green (BG) as well as the reduction of PB to Prussian white (PW). This observation indicates the effective formation of PBNPs onto the surface of the GC electrode. The formal potential was calculated by averaging the cathodic and anodic peak potentials and it is observed as 0.167 V for redox conversion between PB and PW, and 0.819 V for the redox

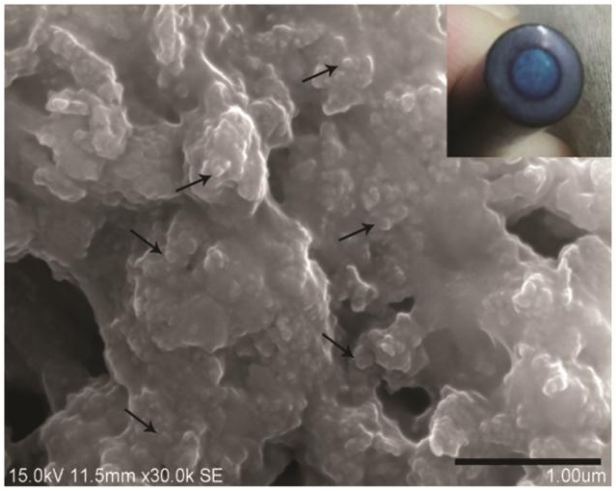

Fig. 5 — FESEM image of APPI(G3)-EH dendrimer stabilized PBNPs.

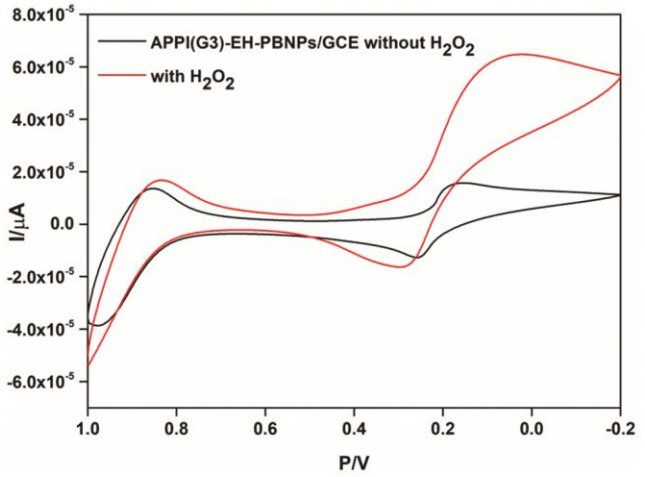

Fig. 6 — Cyclic voltammograms of APPI(G3)-EH-PBNPs/GCE in 0.1M HCl/KCl in the absence and in the presence of 500 μM H_2O_2 at a scan rate of 50 mVs^{-1}.

conversion between PB and BG. These results were found to be in agreement with previous reports[40,41]. The conversion process of the two redox pairs is shown as follows:

$$(PB)\ Fe(III)_4[Fe(II)(CN)_6]_3 + 4e^- + 4K^+ \rightarrow (PW)\ K_4Fe(II)_4[Fe(II)(CN)_6]_3 \quad ...(4)$$

$$(PB)\ Fe(III)_4[Fe(II)(CN)_6]_3 + 3Cl^- \rightarrow (BG)\ Fe(III)_4[Fe(III)(CN)_6]_3Cl_3 + 3e^- \quad ...(5)$$

The surface morphology of PBNPs deposited on the APPI(G3)-EH-Fe^{2+}/GC electrode surface was investigated by field emission-scanning electron microscopy, and the average size of the PBNPs deposited on the electrode was estimated. FESEM results demonstrated that the PBNPs was electrochemically deposited on the surface of the modified electrode with the diameter of about 50-100 nm (Fig. 5). Some larger particles could also be seen on the electrode surface, which seemed to be the accumulation of the PB nanoparticles. These results are in good agreement with those previously reported in literature[42,43].

Electrochemical sensing of APPI(G3)-EH-PBNPs/GCE for H_2O_2

Having established the conditions for the formation of the PB nanoparticles, it is worthwhile to consider this APPI(G3)-EH-PBNPs/GCE for applications in electrocatalysis and electroanalytical chemistry. The importance of nanocomposites in electroanalytical chemistry is obviously due to the inherently high surface-to-volume ratio and the consequent high signal-to-noise ratio that can aid detection at lower concentration levels with good sensitivity. The amphiphilic dendrimer served as a good template for synthesis of PBNPs and thus provide a "platform" for the formation of nanostructured PB. The substrate that has attracted the attention of electrochemists in this context is the reduction of hydrogen peroxide, as its detection is of concern in analytical chemistry and biosensors[44]. It is well-known that the glassy carbon surfaces are highly passive to hydrogen peroxide reduction and hence need to be chemically modified.

In view of the circumstance stated above, it is understood that, though various GCE modified electrode is already available for detection of H_2O_2, still the research on fabricating new GC electrode using sensitive polymeric material for detection and sensing of H_2O_2 is actively continuing. In this piece of study initially, amphiphilic dendrimer based Prussian blue nanoparticles viz., APPI(G3)-EH-PBNPs was prepared and coated the same on GCE through simple electrochemical deposition procedure and thus obtained APPI(G3)-EH-PBNPs/GCE. To check the sensing ability of this electrode with H_2O_2 substrate, initially CV study was conducted for blank medium containing 20 mL of 0.1M KCl prepared using 0.1M HCl keeping the potential range at -0.2 to 1 V *vs* Ag/AgCl with a scan rate of 50 mV/s and subsequently 500 μM of hydrogen peroxide was added into the same medium and electrochemical condition and the CVs were recorded. The obtained CVs for blank and sample solution were shown in Fig. 6.

The electrocatalytic waves for PB nanoparticles on the reduction of H_2O_2 appeared under this condition. From the CVs it is seen that, the peak currents for reduction waves of PBNPs was found to increase

steadily on increasing the [H_2O_2], and the corresponding oxidation peak currents were observed to decreased gradually. The electron transfer occurs in this case mainly by electron hopping (i.e. self-exchange) between neighbouring molecular sites. Further, the large surface area provide by the APPI(G3)-EH dendrimer complex facilitates the formation of more PBNPs on the surface of GCE. This may result in a sensitive APPI(G3)-EH-PBNPs/GC electrode which thus largely attracts the H_2O_2 substrate for reduction. Furthermore, the three-dimensional distribution of PB can obtain large contact area with H_2O_2. As mentioned before, Prussian blue can be electrochemically reduced to Prussian white (PW), which is capable of catalysing the reduction of hydrogen peroxide at low potentials, according to the Equation:

$$(PB)\ Fe(III)_4[Fe(II)(CN)_6]_3 + 4e^- + 4K^+ \rightarrow (PW)\ K_4Fe(II)_4[Fe(II)(CN)_6]_3 \quad ...(6)$$

$$(PW)\ K_4Fe(II)_4[Fe(II)(CN)_6]_3 + 2H_2O_2 \rightarrow (PB)\ Fe(III)_4[Fe(II)(CN)_6]_3 + 4OH^- + 4K^+ \quad ...(7)$$

This reaction shows that the PB nanoparticles serve as an electron-transfer mediator between the APPI(G3)-EH-PBNPs/GCE and H_2O_2. Analogues study reported by Bustos *et al.* for the reduction of H_2O_2 using PAMAM dendrimer stabilized Prussian blue nanoparticles[45]. The current measurements were performed by varying the [H_2O_2] and the obtained CVs indicate that (Fig. 7), at a concentration range from 1-8 mM, an excellent linear relationship was noticed (Fig. 7 inset).

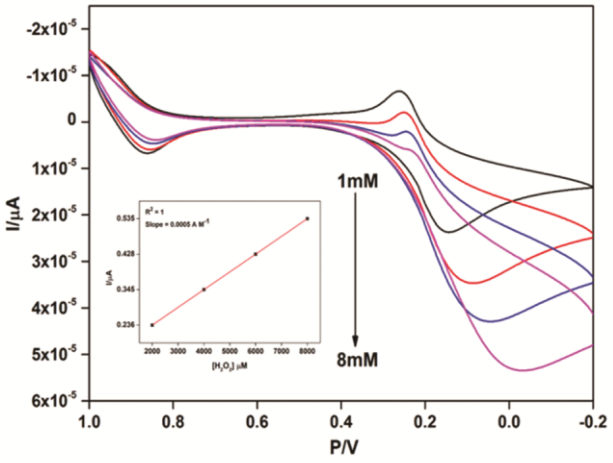

Fig. 7 — Effect of [H_2O_2] on the CV response of APPI(G3)-EH-PBNPs/GCE at a scan rate of 50 mVs^{-1} in 0.1M HCl/KCl (inset : Plot of peak current *versus* [H_2O_2]).

In order to get more information about the catalytic reaction mechanism, CVs were recorded using the APPI(G3)-EH-PBNPs/GCE and by varying the scan rate from 10–200 mV/s by keeping the H_2O_2 concentration as 500 µM. The obtained cyclic voltammograms are shown in Fig. 8, in which the systematic increase in cathodic peak current (i_{pc}) against increase in the scan rate was observed for APPI(G3)-EH-PBNPs/GCE. A Plot of i_{pc} *versus* square root of scan rate ($\upsilon^{1/2}$), result shows that the redox reaction between Prussian blue and Prussian white is observed the plot being linear with a slope of 0.94 (Fig. 8 inset) suggesting that, the electron-transfer reaction was controlled by diffusion.

Further, the APPI(G3)-EH-PBNPs/GCE has also been used as a amperometric sensor for detection of H_2O_2. Figure 9 represents a typical steady state

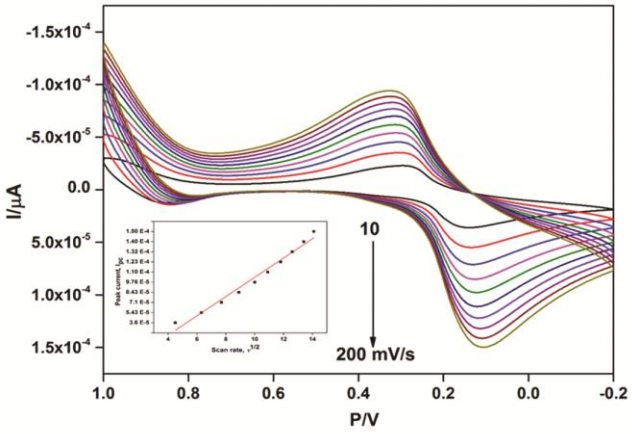

Fig. 8 — Effect of scan rate on the CV response of APPI(G3)-EH-PBNPs/GCE with 500 µM H_2O_2 in 0.1M HCl/KCl. (inset : Plot of peak current *versus* square root of scan rate).

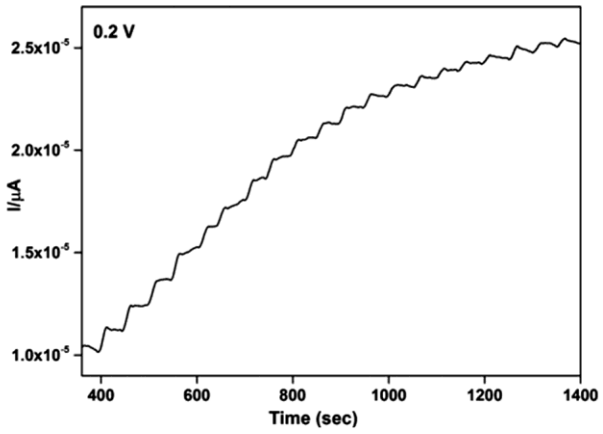

Fig. 9 — Amperometric *i-t* response of APPI(G3)-EH-PBNPs/GCE in 0.1M HCl/KCl at an applied potential of +0.2V *versus* Ag/AgCl, stirring rate ≈ 300 rpm; successive addition of 100 µM H_2O_2 solution.

Fig. 10 — (a) Calibration curve of the amperometric sensor as a function of [H_2O_2] and (b) Interval of linear response in the calibration curve of the sensor.

amperometric response obtained for APPI(G3)-EH-PBNPs/GCE and by periodic addition of H_2O_2. That is, when an aliquot (100 µL) of H_2O_2 was added periodically to the 0.1M HCl and 0.1M KCl, the reduction current was increased sharply and then reaches a steady state value (ca. 95%) in less than 10 s. To obtain the calibration curves for APPI(G3)-PBNPs/GC electrode, the steady state current values were plotted with [H_2O_2].

Figure 10(a) illustrates the calibration curve obtained for variation of [H_2O_2], and Fig. 10(b) shows the linear range of the calibration curve. The linear relationship has been obtained in the concentration range of 100 to 1000 µM ($r^2 = 0.95$) with a sensitivity of 0.012 AM^{-1} and the detection limit is observed as 60 µM at a signal-to-noise of 3. The synergistic effect between PB and APPI(G3)-EH is responsible for effective detection of hydrogen peroxide.

Concerning the APPI(G3)-PBNPs/GC electrode response, the interferences from the coexisting ascorbic acid and uric acid could be neglected, owing to the low applied potential (0.2 V). Therefore, based on the results and explanations we have arrived at a logical conclusion that the APPI(G3)-EH-PBNPs nanostructured coating material may largely interest electrochemists to design/fabricate a new sensitive electrode for effective detection of H_2O_2 especially at low potentials.

Conclusion

Novel amphiphilic poly(propylene imine) dendrimer template (APPI(G3)-EH) has been developed by chemical modification of PPI(G3) with 1,2-epoxyhexane. The functionalization of 1,2-epoxyhexane onto the peripheral primary amines of PPI(G3) has been confirmed using FT-IR, ^{1}H NMR and ^{13}C NMR techniques. The APPI(G3)-EH is used as a template for encapsulation of PBNPs which produced homogeneous APPI(G3)-EH-PBNPs catalyst. The catalyst has been characterized with SEM and CV techniques. The newly fabricated APPI(G3)-EH-PBNPs-GC electrode is proved to be sensitive enough to sense/detect the H_2O_2 to the tune of 100 to 1000 µM with a sensitivity of 0.012 AM^{-1} and the detection limit of 60 µM. Therefore, the study confirms that APPI(G3)-EH-PBNPs is a catalyst for promising application in the field of sensors.

Acknowledgement

The authors are grateful for the support provided by Department of Physical Chemistry, University of Madras, Chennai and CMRIT, Bangalore for this work.

References

1 Qiu W, Zhua Q, Gao F, Gao F, Huang J, Pan Y & Wang Q, *Mat Sci Eng C*, 72 (2017) 692.
2 Cutler R G, Camandola S, Malott K F, Edelhauser M A & Mattson M P, *Curr Top Med Chem*, 15 (2015) 2233.
3 Tomczynska M, Bijak M & Saluk J, *Curr Top Med Chem*, 16 (2016) 2223.
4 Ojani R, Hamidi P & Raoof J B, *Chin Chem Lett*, 27 (2016) 481.
5 Lee J H,Tang I N & Weinstein-Lloyd J B, *Anal Chem*, 62 (1990) 2381.
6 Hanaoka S, *Anal Chim Acta*, 426 (2001) 57.
7 Fernandes E, Gomes A & Lima J L F C, *J Biochem Biophys Methods*, 65 (2005) 45.
8 Nogueira M C O R F P & Paterlini W C, *Talanta*, 66 (2005) 86.
9 Wang J, *Biosens Bioelectron*, 21 (2006) 1887.
10 Prabhu P, Babu R S & Narayanan S S, *J Solid State Electrochem*, 18 (2014) 883.
11 Manusha P, Theyagarajan K, Elancheziyan M, Shankar H, Thenmozhi K & Senthilkumar S, *ECS Sensors Plus*, 1 (2022) 033601.

12 Murphy M, Theyagarajan K, Thenmozhi K & Senthilkumar S, *Colloids Surf. B: Biointerfaces*, 199 (2021) 111540.
13 Murphy M, Theyagarajan K, Thenmozhi K & Senthilkumar S, *Electroanalysis*, 32 (2020) 2422.
14 Nagarajan R D, Sundaramurthy A & Sundramoorthy A K, *Chemosphere*, 286 (2022) 131478.
15 Shanmugam P, Rajakumar K, Boddula R, Ngullie R C, Wei W, Xie J & Murugan E, *Mater Sci Energy Technol*, 2 (2019) 532.
16 Murugan E, Nimita J J, Ariraman M, Rajendran S, Janankiraman K, Akshata C R & Kalpana K, *ACS Omega* 3 (2018) 13685.
17 Shanmugam P P, Wei W, Xie J & Murugan E, *Asian J Chem*, 31 (2019) 235.
18 Murugan E & Kalpana K, *Adv Mater Proc*, 3 (2018) 75.
19 Murugan E, Rubavathy Jaya Priya A, Janaki Raman K, Kalpana K, Akshata C R, Santhosh Kumar S & Govindaraju S, *J Nanosci Nanotechnol*, 19 (2019) 7596.
20 Murugan E & Pakrudheen I, *Sci Adv Mater*, 6 (2014) 1.
21 Murugan E & Pakrudheen I, *Appl Catal A: General*, 439 (2012) 142.
22 Murugan E, Rangasamy R & Pakrudheen I, *Sci Adv Mater*, 4 (2012) 1103.
23 Pakrudheen I, Banu A N & Murugan E, *Environ Chem Lett*, 16 (2018) 1513.
24 Shahvandi S K, Ahmar H & Rezaei S J T, *Surf Inter*, 12 (2018) 71.
25 Elancheziyan M, Theyagarajan K, Saravanakumar D, Thenmozhi K & Senthilkumar S, *Mater Today Chem*, 16 (2020) 100274**.**
26 Baghayeri M, Alinezhad H, Tarahomi M, Fayazi M, Ghanei-Motlagh M & Maleki B, *Appl Surf Sci*, 478 (2019) 87.
27 Jiang T, Zhan D & Chen Y, *Ferroelectrics*, 580 (2021) 42.
28 Yang L, Wang J, Lü H & Hui N, *Microchim Acta*, 188 (2021) 25.
29 Chen J, Yu Q, Fu W, Chen X, Zhang Q, Dong S, Chen H & Zhang S, *Sensors*, 20 (2020) 2924.
30 Zhang M, Zhang W, Engelbrekt C, Hou C, Zhu N & Chi Q, *Chem Electro Chem*, 7 (2020) 3818.
31 Ma F, Ge G, Fang Y, Ni E, Su Y, Cai F & Xie H, *New J Chem*, 45 (2021) 962
32 Ni P, Zhang Y, Sun Y, Shi Y, Dai H, Hu J & Li Z, *RSC Adv*, 3 (2013) 15987.
33 Zhu Z, Gong L, Miao X, Chen C & Su S, *Biosensors*, 12 (2022) 260.
34 Zhang C, Brien S O & Balogh L, *J Phys Chem B*, 106 (2002) 10316.
35 Wang C, Zhang L, Guo Z, Xu J, Wang H, Shi H, Zhai K & Zhuo X, *J Electroanalysis*, 22 (2010) 1867.
36 Fang B, Feng Y, Wang G, Zhang C, Gu A & Liu M, *Microchim Acta*, 173 (2011) 27.
37 Yang D J, Hsu C Y, Lin C L, Chen P Y, Hu C W, Vittal R & Ho K C, *Energy Mater Solarcells*, 99 (2012) 129.
38 Karyakin A A & Karyakin E E, *Sens Actuator B: Chem*, 57 (1999) 268.
39 Yang C, Wang C H, Wu J S & Xia X H, *Electrochim Acta*, 51 (2006) 4019.
40 Itaya K, Ataka T & Toshima S, *J Am Chem Soc*, 104 (1982) 4767.
41 Karyakin A A, *Electroanalysis*, 13 (2001) 813.
42 Salasar P, Martin M, O'Neill R D, Roche R & Gonzalez-Mora J L, *J Eletroanal Chem*, 674 (2012) 48.
43 Jiang Y, Zhang X, Shan C, Hua S, Zhang Q, Bai X, Dan L & Niu L, *Talanta*, 85 (2011) 76.
44 Karyakin A A, Puganova E A, Budashov I A, Kurochkin I N, Karyakina E E & Levchenko V A, *Anal Chem*, 76 (2004) 474.
45 Bustos E & Godínez L A, *Int J Electrochem Sci*, 6 (2011) 1.